Phys. Status Solidi A **212,** No. 10, 2107–2113 (2015) / **DOI** 10.1002/pssa.201532272

physica status solidi a
www.pss-a.com
applications and materials science

Additively-manufactured piezoelectric devices

David I. Woodward*[,1], Christopher P. Purssell[2], Duncan R. Billson[2], David A. Hutchins[2], and Simon J. Leigh[2]

[1] Department of Physics, University of Warwick, Gibbet Hill Road, Coventry CV4 7AL, UK
[2] School of Engineering, University of Warwick, Library Road, Coventry CV4 7AL, UK

Received 12 April 2015, revised 29 June 2015, accepted 6 July 2015
Published online 28 July 2015

Keywords ceramics, piezoelectricity, stereolithography, transducers, ultrasound

* Corresponding author: e-mail d.i.woodward@warwick.ac.uk, Phone: +44 (0)24 7658 4589, Fax: +44 (0)24 7666 7224

This is an open access article under the terms of the Creative Commons Attribution License, which permits use, distribution and reproduction in any medium, provided the original work is properly cited.

A low-cost micro-stereolithography technique with the ability to additively manufacture dense piezoelectric ceramic components is reported. This technique enables the layer-wise production of functional devices with a theoretical in-plane resolution of ~20 μm and an out-of-plane resolution of <1 μm without suffering a significant reduction in the piezoelectric properties when compared to conventionally produced ceramics of the same composition. The ability to fabricate devices in complex geometries and with different material properties means that conventional limits of manufacturing are not present. A hollow, spherical shell of the piezoelectric material $0.65Pb(Mg_{1/3}Nb_{2/3})O_3$–$0.35PbTiO_3$, built without tooling or recourse to additional equipment or processes, is shown generating ultrasound in the MHz range.

1 Introduction Piezoelectric ceramics are used for a wide range of technological applications that include ultrasound transducers for naval, medical and nondestructive evaluation applications, fuel injectors for diesel engines and cantilevers for harvesting energy from ambient vibrations [1]. The shape and geometry of piezoelectric ceramics can directly influence their functional properties. For example, an array of ceramic pillars in a polymer matrix (known as a 1–3 piezocomposite) can be used to create an ultrasound transducer with lower acoustic impedance and higher electromechanical coupling factors than a simple slab of ceramic [2]. Conventional manufacturing of such 1–3 piezocomposites is achieved by the 'dice and fill' technique: cutting channels into ceramic blocks and then back-filling the channels with a suitable polymer [3]. However, the resulting regular array of ceramic elements allows standing waves to develop in the plane of the transducer. These resonances couple to the resonant frequency in the transducer thickness direction and degrade performance. Although it is possible to cut the channels in such a way as to generate a pseudo-random distribution of elements that reduces standing waves within the transducer [4], the fabrication mechanism imposes a severe limit on the ability to make further geometric modifications.

Having greater freedom in achievable geometry can potentially offer significant improvements in the performance of many devices, including 1–3 piezocomposites, in particular the use of wider bandwidths and shorter pulse lengths [5], but further shaping of devices is an energy- and time-intensive processing step. Injection moulding techniques have enabled rapid production of high-volume devices [6] and techniques such as tape-casting [7] and gel-casting [8] have made it possible to create devices that could not be made by conventional methods, and yet all of these techniques remain far from widespread, due in part to the high initial costs and the potential restrictions these techniques place on the build process, for example, the need to first create an accurate mould for injection moulding or gel-casting. Thus, in order to access and explore more advanced properties of piezoelectric ceramics and improve the capabilities of all piezoelectric devices, there is a clear need for a low-cost technique that will allow the rapid production of new and complex geometries without the need for new tooling for every change in design.

Additive manufacturing (AM) encompasses several techniques where solid objects are built up in a layer-by-layer process by depositing material only where it is required. As a group of processes, they are distinct from more traditional subtractive manufacturing techniques such as milling, machining and drilling. AM is a rapidly developing area where the enhanced freedom in geometric

© 2015 The Authors. *Phys. Status Solidi A* published by WILEY–VCH Verlag GmbH & Co. KGaA, Weinheim

construction inspires new approaches in the design of products and devices and can offer a route to the simplified and rapid manufacture of complex piezoelectric structures such as helixes [7], springs [9], accordions [10] and flexoelectric structures [11] that have valuable functions but currently require highly specialised fabrication processes. To enable AM to change the future of designing and building ceramic devices, a truly widespread technique is required; one that is low-cost but has high accuracy and resolution and can be applied to the widest possible range of piezoelectric materials. Five principal technologies exist for AM of ceramics [12]: (i) laser sintering of ceramic powders, (ii) printing of binder onto ceramic powder, (iii) stacking and bonding of laser-cut ceramic plates, (iv) extrusion of ceramic-loaded paste and (v) photocuring of ceramic-loaded resins. Of these, (i) and (iii) employ high-power lasers, requiring high capital investment and necessitating complex software, whereas (iv) is unsuited to the accuracy and resolution required for a large proportion of piezoelectric devices.

The AM technology chosen for this study was curing of ceramic-loaded photo-sensitive resins using micro-stereolithography (MSL). It combines low capital and operating cost with simplicity, high resolution and the potential to be applied to a wide variety of materials [13]. The use of engineering materials such as silica [14] and alumina [15] has previously been demonstrated using a scanning ultraviolet (UV) laser to cure thin lines in separate layers. The resulting green body typically contains 40–60 vol% ceramic powder and is heated to burn out the organic components and sinter the remaining powder [16, 17]. This process is capable of building parts with a resolution of the order of tens of microns [18].

There have been far fewer studies of the stereo-lithography of ferroelectric materials in suspension. The scattering of light due to the large difference in refractive index between the resin and the ceramic particles, in addition to light absorption, appears to have limited previous studies into $BaTiO_3$ [19] and $Pb(Zr,Ti)O_3$ (PZT) [20] due to the resulting shallow cure depth. Singh et al. [16] demonstrated an MSL technique for building piezoelectric ceramics that used UV light to cure a 40 vol% suspension of PZT and a single glass mask to define the size and shape of the cured regions. However, there are several drawbacks to these technologies: UV lasers present hazards related to skin and eye exposure and, as point sources, are not ideal for curing larger areas of material. The UV light with glass mask is a system that is much more suited to curing larger areas, but the use of a physical mask means that a new mask must be created whenever the shape of the cured area is to change. Most importantly, however, none of these studies have shown the properties of the resulting ceramics and how they would compare to conventionally formed ceramics.

This paper presents the development of a photocurable MSL resin containing $0.65Pb(Mg_{1/3}Nb_{2/3})O_3$–$0.35PbTiO_3$ (PMNT), a material with one of the highest known piezoelectric coefficients, d_{33}, of all electroceramics [21] and the subsequent production of green bodies with a range of structures which, upon sintering, maintain their shapes and structures while undergoing reproducible shrinkage and possessing physical properties that are as close as possible to those of conventionally formed ceramics of the same composition.

2 Experimental For this work, we have created an MSL platform which follows the same design principles as one used to build a miniature flow sensor, using a photocurable resin loaded with Fe_3O_4 particles [13]. A photocurable liquid sits in a transparent resin tray and a build platform with a flat glass substrate mounted parallel to the bottom of the resin tray moves down into the resin until a thin layer remains between the build platform and the resin tray. This thin layer is illuminated with a light source that consists of a simple bundle of three LEDs delivering red, green and blue light centred on wavelengths 628, 519 and 462 nm, respectively. The light is reflected up into the resin by a digital micro-mirror device (DMD), which allows the shape of each cured layer to be defined. Once cured, the resin tray is peeled off the cured layer, the build platform with the cured layer attached moves up and fresh resin flows back into the void previously filled by the cured layer. The process then restarts for the second layer and continues until the desired object has been built. In contrast to using a single point laser to cure the polymer resin, the use of a projection system enables the parallel manufacture of extra 3D parts, potentially with no impact on manufacturing time.

This MSL platform has been designed to work with viscous resins and to offer maximum control over the build parameters. The layer thickness can be altered with a resolution of 1 μm, and the DMD controls the pattern of the light that reaches each layer to a resolution of 25 μm. Complex shapes can be built up within an X–Y build envelope of approximately 18 mm × 32 mm. Other parameters that can be changed include colour mix and intensity, illumination time, resin tray peel speed and build platform raising and lowering speeds.

The MSL process required a suspension containing a powder within a suitable photocurable resin. A mixture of 65 mol% $Pb(Mg_{1/3}Nb_{2/3})O_3 + 35$ mol% $PbTiO_3$ powder was obtained from Ecertec Ltd. (UK) and was reacted in an alumina crucible at 850 °C for 4 h and milled for 24 h with 1 cm diameter zirconia milling media in propan-2-ol. An organic dispersant, Triton X-114 (Sigma–Aldrich), was added prior to milling so that the volume ratio of PMNT: Triton was 2:1. The slurry was subsequently dried at 70 °C and then ground with a pestle and mortar before being passed through a 250 μm sieve.

It was found that the exact composition of the powder/resin mixture was very important to allow the resultant suspension to perform properly in the MSL process. There were various factors that affected the ability to cure the resin and allow proper manufacture to take place. For example, light scattering from the powder had an effect on the curing

© 2015 The Authors. *Phys. Status Solidi A* published by WILEY–VCH Verlag GmbH & Co. KGaA, Weinheim

process and the density and viscosity of the resin had to be considered. Experimentation found that a suitable photocurable resin consisted of 0.94 ml of 1,6-hexanediol diacrylate (HDDA) and 0.77 ml of dipentaerythritol penta-/hexa-acrylate (DPPHA). 15 g of the PMNT/Triton mixture was then added to this resin while stirring and heating to 45 °C. Finally, 0.03 g of Irgacure 784 (BASF) photoinitiator was added to facilitate photocuring. This formulation produced a resin containing approximately 40% PMNT by volume that had appropriate flow properties for MSL use.

There are adjustable variables within the MSL process, including the individual layer thickness and illumination properties. It was found that suitable green bodies were produced by photocuring the resin in 50 μm thick layers using illumination with white light (all three LEDs active) for 60 s. The resulting parts were cleaned in acetone, placed in alumina crucibles with a covering of PMNT powder to prevent lead loss and sintered in a Lenton AWF 13/5 furnace. The parts were heated at 1°/min to 600 °C and then held at this temperature for 1 h to burn out all of the organic components. They were then heated at 3°/min to 1250 °C and held for 1.5 h for the densification stage, followed by cooling at 3°/min. For the purposes of comparison, ceramics were made from the PMNT/Triton mixture by a conventional route, pressing 13 mm diameter pellets using a load of 1 tonne and sintering via the same process.

The dimensions and masses of green bodies and ceramics were recorded and the volumes of both were obtained by measuring the change in mass on immersing into distilled water. Scanning electron microscopy (SEM) was performed on green bodies and ceramics using a Zeiss Supra 55-VP operating at 10 kV. Dielectric permittivity and loss of ceramics were measured using an HP 4192A LF Impedance Analyser using a heating rate of 60 °C h^{-1}. Poling of pellets was performed in silicone oil at room temperature by applying a fixed voltage of 1 kV mm^{-1} for 1 min. Measurements of d_{33} were made for five points on both surfaces of the pellets using a YE2730A d_{33} meter (APC International, Ltd.). Dielectric hysteresis was performed using a triangular waveform at a frequency of 50 mHz.

Ceramics were used to generate an ultrasound signal using a Panametrics Pulser Receiver Model 5055PR to excite the transducer. A Polytec OFV 5000 laser vibrometer was used to measure surface movement. A needle hydrophone was used to measure peak intensity of the received signal when immersed in water.

3 Results and discussion A range of resins with different PMNT loadings were made. The optimum loading gave a resin with a suitably low viscosity for MSL, and, once sintered, yielded ceramics with densities close to those of conventionally formed ceramics. The green bodies obtained from the optimum loading were found to have densities of 4.18(3) g cm^{-3}, corresponding to a PMNT loading of 42.5 (5) vol%. Lower loadings were found to result in ceramics with densities <95% of the theoretical maximum, as obtained from the molecular mass and previous refinements of the unit cell volume [22], and while producing such ceramics with greater porosity is often not desirable, it is a feature that can have useful benefits. SEM images of green composites showed undulations at the sides of the green bodies that originate from light scattered horizontally (Fig. 1a), probably exacerbated by scattering by the high refractive index particles. In the green body, the undulations at each side were found to add ~40 μm of width approximately half-way between the layer interfaces. SEM studies showed no evidence of the particles settling or clustering within each layer or at the interfaces between layers, indicating a homogeneous distribution of particles in the green bodies and, by implication, within the resin. The earliest samples produced for this study without dispersant were found by SEM to exhibit particle clustering, resulting in a layered structure alternately rich and deficient in particles. The subsequent use of dispersant was found to have a clear benefit towards the homogenisation of the particles within the liquid phase. SEM imaging of green bodies formed within the MSL process shows that the particles were mostly sub-micron in size (Fig. 1b).

Photographs of a square PMNT piezoelectric element are shown in Fig. 1c in both green and post-sintered ceramic form. MSL ceramics were typically fabricated to a thickness of 1.5 mm and width of 6 mm and densities of 7.98(6) g cm^{-3}, corresponding to 97.8(7)% of the theoretical maximum. By comparison, the conventionally produced ceramics had densities of 8.03(2) g cm^{-3}, corresponding to 98.4(2)% of the theoretical maximum. The slightly lower density of the MSL ceramics may result from the lower packing density of particles in the MSL resin than in the green bodies formed under uniaxial pressure. Shrinkage on sintering was found to be 25.5(4)% in the direction perpendicular to the layers and 24.0(4)% within the layers. Taking into account the pixel size of the DMD and the accuracy of the vertical movement of the stage, ceramics can theoretically be made with a resolution of approximately 20 μm in the X–Y plane and <1 μm in the vertical direction.

The sintered MSL ceramics were examined by SEM (Fig. 1d–f). Minimal distortion of the object takes place on sintering, as evidenced by the layer interfaces remaining straight, although some distortion is observed in parts where the width:thickness ratio is very high, indicating that further improvements to the resin formulation and processing conditions may be possible. The undulations between the layer interfaces observed at the edges of the composites are retained in the sintered body, while dark zones were observed to occur between the layers. These are gaps between MSL fabrication layers that extend only a short distance (up to 100 μm) into the body of the ceramic (Fig. 1e), indicating that the layer-by-layer build-up of material does not cause delamination within the main body of the final ceramic. Figure 1f shows the grain structure, which is well-packed with minimal gaps, indicating that the

© 2015 The Authors. *Phys. Status Solidi A* published by WILEY–VCH Verlag GmbH & Co. KGaA, Weinheim

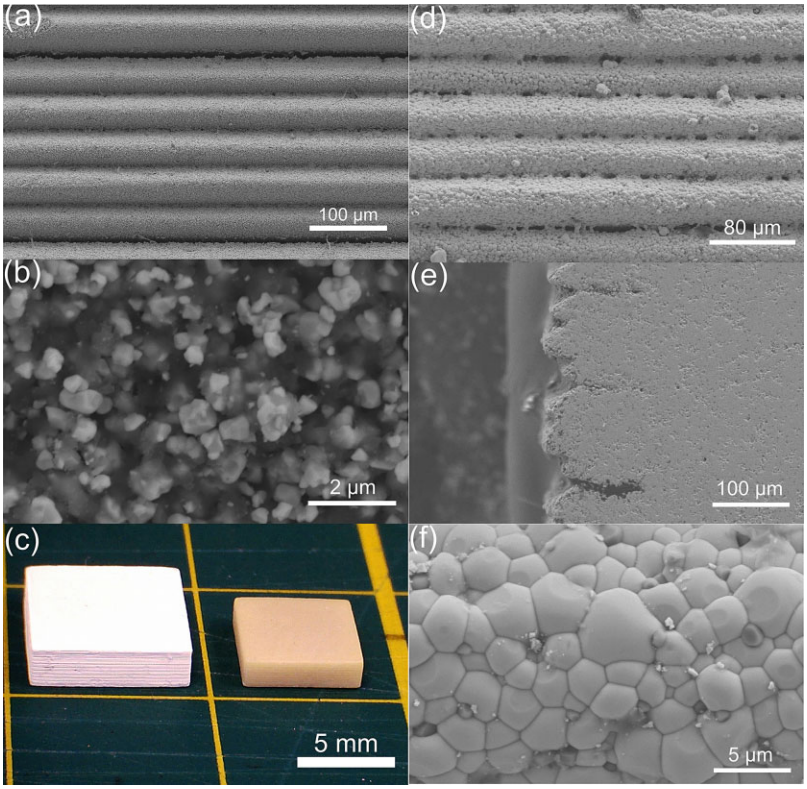

Figure 1 Secondary electron images of (a) the side of a green body, viewed parallel to the layers. The interfaces between several layers can be clearly seen due to the bulging that results from light scattering during curing, (b) PMNT particles within the polymer matrix, (c) photograph of a square ceramic element in both green composite form (left) and corresponding sintered ceramic (right) with thickness 1.5 mm. Secondary electron images of an MSL ceramic showing (d) the appearance of the side of the sample, showing the undulations formed around the perimeter of each layer, (e) a section through the material, indicating that layering only penetrates a short distance into the structure, and (f) the grain structure at higher magnification.

sintering has produced high-quality ceramics. In addition, the mean grain diameter is ~2 μm, demonstrating that significant grain growth has taken place on sintering.

The d_{33} was measured for five separate MSL ceramics and compared to the values obtained from five ceramics made using the conventional technique. Poling was performed at 1.0 kV mm^{-1} for both sets of samples. The d_{33} of the MSL ceramics measured on faces parallel to the deposited layers was 620(40) pC N^{-1}, while the d_{33} of the conventional ceramics was 630(50) pC N^{-1}. These particularly close values indicate that a similar performance can be expected from ceramics fabricated by both routes. A more detailed study of the d_{33} was made by varying the poling voltage (Fig. 2a). This also shows that the piezoelectric properties of ceramics made by the two routes are very similar. However, unlike the conventional ceramic, the d_{33} of the MSL ceramic is not fully reversible. The d_{33} when fully poled is 636(26) pC N^{-1}, but when reversed, it is −618(34) pC N^{-1}. Similar behaviour has been observed in $Pb(Zr,Ti)O_3$ and $Na_{½}Bi_{½}TiO_3$ ceramics and assigned to polarisation pinning by defects [23, 24]. In the case of the PMNT ceramics presented here, the effect is relatively slight and may simply reflect the slightly higher porosity of the MSL ceramics.

Hysteresis loops (Fig. S1, Supporting Information, see online at: www.pss-a.com) and measurements of dielectric permittivity and loss at a fixed frequency of 100 kHz (see Supporting Information, Fig. S2) were obtained for both types of ceramic. The hysteresis loops show that the MSL ceramics have slightly lower remnant polarisation and slightly higher coercive field than the ceramics prepared by the coventional method, while the dielectric data show that the conventionally produced ceramics have sharper peaks in both dielectric permittivity and loss. All of these effects are attributable to the difference in porosity in the two materials, but crucially, indicate only a small difference in performance.

The impulse response of a poled MSL ceramic was measured by driving a square element with a large voltage step, in this case 200 V, and measuring the surface movement optically with a laser vibrometer normally incident on the flat face of the ceramic. The Fourier transform of the signal (Fig. 2b) reveals a dominant frequency at ~1.1 MHz, a value that is particularly close to that expected for an undamped PMNT ceramic of thickness 1.5 mm vibrating in the thickness mode [1].

To investigate the influence of the layer-wise build-up on the piezoelectric properties of the ceramics, a cube with edges 3.6 mm was printed and sintered. Poling with a field of 1 kV mm^{-1} applied perpendicular to the layers resulted in a d_{33} of 645(18) pC N^{-1}, while a field of equal magnitude applied parallel to the layers resulted in a d_{33} of 576(40) pC N^{-1}. After removing 150 mm of material from these two faces, repoling with the same field strength resulted in a d_{33} of 629(15) pC N^{-1}. The four faces of the cube that were formed perpendicular to the deposited layers exhibited a serrated structure due to the scattering of light within the individual layers and this appears to have an effect of reducing the apparent d_{33} of the poled ceramic.

© 2015 The Authors. *Phys. Status Solidi A* published by WILEY–VCH Verlag GmbH & Co. KGaA, Weinheim

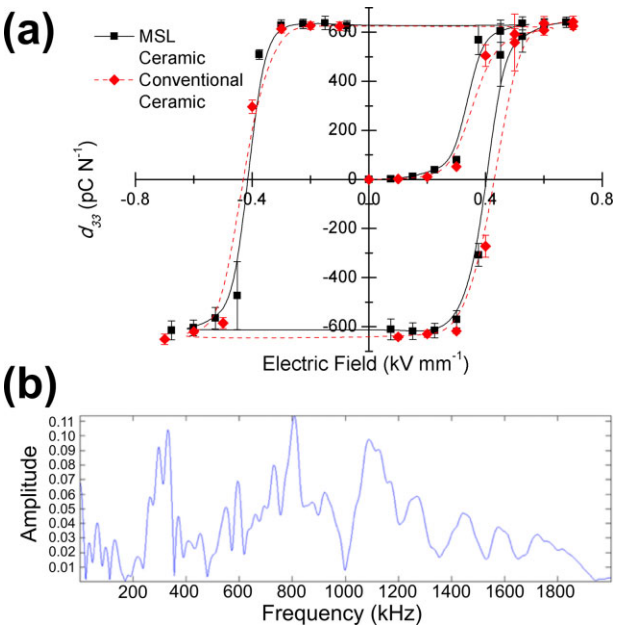

Figure 2 (a) Loop of *ex situ* d_{33} obtained for MSL and conventional ceramics as a function of poling field, (b) frequency spectrum of the ultrasonic impulse response for a rectangular PMNT ceramic of thickness 1.5 mm fabricated using MSL, showing the frequency spectrum.

This macroscopic anisotropy in d_{33} could be exploited in the manufacture of piezoelectric arrays, as the effect would be to reduce cross-coupling between array elements.

Piezoelectric ceramics are used in many different media for a wide range of applications, such as imaging and flow measurement. In order to test both the geometric capability of the ceramic MSL process and the functionality of the resultant poled ceramic in a piezoelectric application, a structure was designed and produced that could be easily characterised for its ability to produce ultrasound, yet would prove challenging to make by existing methods. Hollow spheres are valuable for ultrasonic applications such as hydrophones where an omnidirectional response is required. Solid slabs of piezoelectric ceramics are of little practical use as the charge formed under applied hydrostatic pressure is particularly small, due to the longitudinal and transverse piezoelectric coefficients being of opposite sign [25], while solid spheres have much lower sensitivity than the hollow versions [26] and cannot be poled or actuated radially. The exact waveform emitted by the device depends on both the material properties and physical properties such as dimensions, shape and mounting constraints. Existing methods of making miniature hollow spheres include blowing bubbles with a PZT-loaded slurry that is subsequently sintered [27]. Such a process is extremely specialised and does not lend itself easily to additional featuring or modification such as producing an oval device, while conventional, subtractive machining would be an uneconomical process for creating such a small and intricate structure.

A hollow, spherical structure was designed so that after sintering, it would have an equatorial diameter of 9.5 mm and a wall thickness of 1 mm. The top and bottom of the sphere had an equal amount sliced off to allow for ease of adding electrodes and give a post-sintering height of 5.25 mm. A disc was added to the base of the part to assist in adhering it to the build platform. The entire model was then 'sliced' to 150 cross-sectional images for consecutively curing the resin in 50 μm layers. After manufacture, the green body was sintered to yield the dense ceramic. After the base was ground off, contacts were added to the internal and external faces using silver paint and the sphere was poled radially using a voltage of 1.3 kV applied for 1 min. The sphere was mounted in a water immersion tank and driven with a voltage impulse to generate ultrasound (Fig. 3a). The ultrasound signal was received at a standoff (minimum separation between hydrophone tip and sphere) of 3 mm and Fourier transform analysis of the recorded signal yielded a main operating frequency of 2.8 MHz (Fig. 3b). A contour plot of the peak amplitude of the received signal in the *X*–*Y* plane (Fig. 3c) showed a maximum intensity at the centre of the field with signal intensity dropping towards the outer area of the field, matching the curve of the transducer face. Horizontal bands of reduced intensity towards the top and bottom of the signal amplitude maps correspond to the top and bottom surfaces of the sphere. Such an intensity distribution in a single plane may have uses as a means of distributing ultrasonic energy over a wide volumetric area, for example in underwater sensing applications.

While the spherical shell is not impossible to produce by alternative machining routes, here we have demonstrated that a proof-of-concept device can be designed, realised and operated in a very short time, without the need for new tooling or the use of additional processes beyond the stereolithography developed here. A recent study employing a zirconia-loaded resin gives some excellent examples of the complexity of structures that this technique can be used to produce [28]. With this capability of geometric control, it becomes simple and rapid to explore new modes of transducer operation. The spherical shell demonstrated here could be used to generate ultrasound at specific frequencies, but the possibilities go far beyond. Pulsing of the sphere can also be used to pump fluids or generate sonoluminescence. The stereolithography process can be used to generate arrays of piezoelectric pillars for 1–3 piezocomposites, but these can be of any shape, e.g. circles, ellipses, pentagons, chosen to minimise crosstalk between pillars. They can be arranged completely randomly, to minimise standing waves and they need not be flat, so they can be built to conform to curved surfaces. Other devices, such as flexoelectric, truncated pyramids [11] or flextensional transducers [29] can also be built without the same heavy restrictions on geometry that have always been imposed on their construction. Lead-free piezoelectric materials where the piezoelectric coefficients are generally inferior to those of lead-based materials can be built with structures that enhance their functional properties for specific applications [30]. With the adoption of this

© 2015 The Authors. *Phys. Status Solidi A* published by WILEY–VCH Verlag GmbH & Co. KGaA, Weinheim

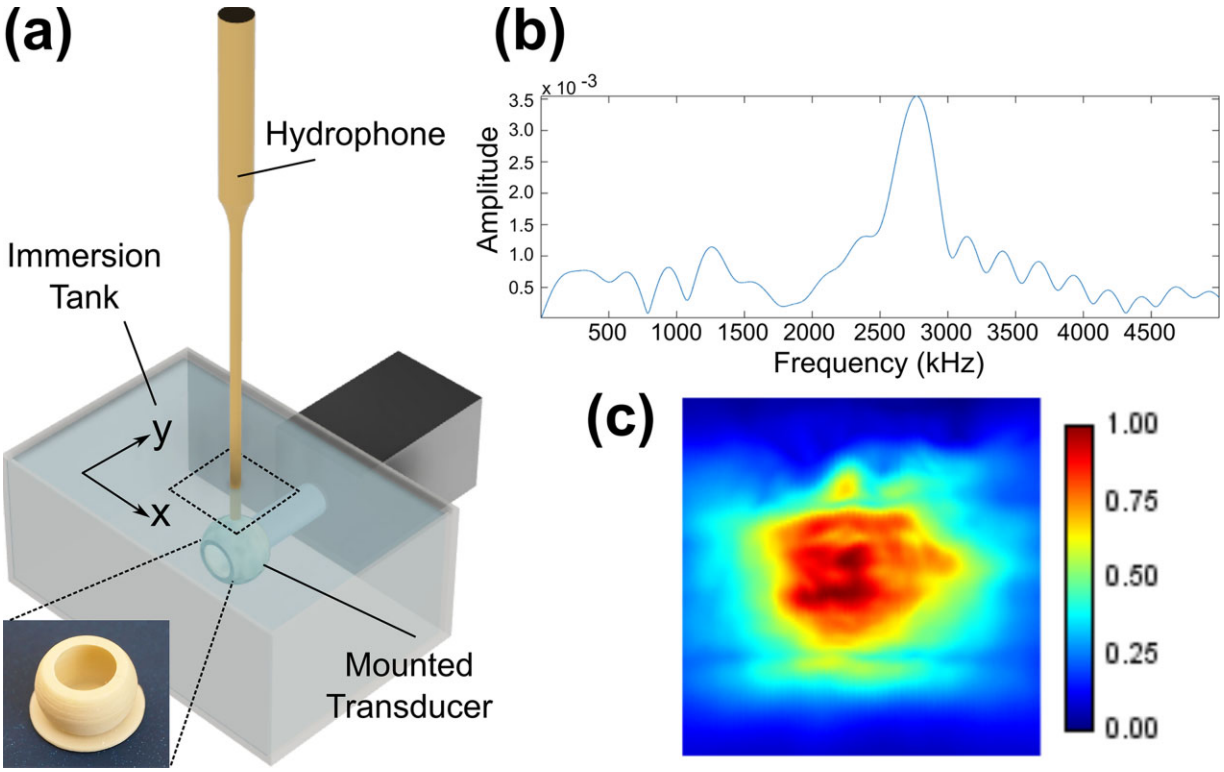

Figure 3 The hollow, spherical ceramic shell performing as an ultrasonic transducer: (a) schematic of the experimental apparatus, (b) Fourier transform of the received signal showing the dominant frequency at 2.8 MHz, (c) contour plot of the peak signal amplitude recorded in the *X*–*Y* plane by the hydrophone at 3 mm standoff.

low-cost technology, the ability to create complex functional devices can be available as a standard laboratory tool for all material scientists and engineers.

4 Conclusions A low-cost stereolithography process for the additive manufacturing of piezoelectric ceramics has been developed and used to build ceramics of the high-d_{33} ferroelectric $0.65Pb(Mg_{1/3}Nb_{2/3})O_3$–$0.35PbTiO_3$. The sintered ceramics are shown to have the high densities necessary for use in applications and their physical properties are shown to be extremely close to those of ceramics prepared conventionally using uniaxial pressure. The process lends itself to flexibility in terms of shapes, sizes and changes in materials. To prove the applicability of this process to the construction of functional devices, a hollow spherical shell was designed and built, poled radially and recorded emitting ultrasound in the MHz range.

Supporting Information

Additional supporting information may be found in the online version of this article at the publisher's website.

Acknowledgements This work was partly funded by the Higher Education Funding Council for England (HEFCE) under the HEIF-5 Impact Fund, and the Engineering and Physical Sciences Research Council (UK), via the UK Research Centre for Nondestructive Evaluation (RCNDE). Thanks are due to Connor Watts and Rui Wang for assistance with sample preparation.

References

[1] J. Holterman and P. Groen, An Introduction to Piezoelectric Materials and Applications, Stichting (Applied Piezo, Apeldoorn, Netherlands, 2013).
[2] W. A. Smith, A. Shaulov, and B. A. Auld, Proc. IEEE Ultrason. Symp., p. 642 (1985).
[3] T. R. Howarth and R. Y. Ting, IEEE Trans. Ultrason. Ferroelectr. Freq. Contr. **47**, 886 (2000).
[4] H.-C. Yang, J. Cannata, J. Williams, and K. K. Shung, IEEE Trans. Ultrason. Ferroelectr. Freq. Contr. **59**, 2312 (2012).
[5] T. A. Whittingham, Eur. Radiol. **9** (Suppl. 3), S298 (1999).
[6] D. Fiore, R. Gentilman, H. Pham, W. Serwatka, P. McGuire, and L. Bowen, Proc. Tenth IEEE Int. Symp. Appl. Ferro., p. 531 (1996).
[7] D. H. Pearce, A. Hooley, and T. W. Button, Sens. Actuators A **100**, 281 (2002).
[8] L. García-Gancedo, S. M. Olhero, F. J. Alves, J. M. F. Ferreira, C. E. M. Demoré, S. Cochran, and T. W. Button, J. Micromech. Microeng. **22**, 125001 (2012).
[9] D. Kim, S. Hong, D. Li, H. S. Roh, G. Ahn, J. Kim, M. Park, J. Hong, T.-H. Sung, and K. No, RSC Adv. **3**, 3194 (2013).
[10] M. Wagner, A. Roosen, H. Oostra, R. Hoeppener, M. de Moya, D. H. Pearce, and T. Hooley, J. Europ. Ceram. Soc. **25**, 2463 (2005).

© 2015 The Authors. *Phys. Status Solidi A* published by WILEY–VCH Verlag GmbH & Co. KGaA, Weinheim

[11] L. E. Cross, J. Mater. Sci. **41**, 53 (2006).
[12] P. Reeves, Rapid Manufacturing for the Production of Ceramic Components (Econolyst Ltd., Wirksworth, UK, 2008).
[13] S. J. Leigh, C. P. Purssell, J. Bowen, D. A. Hutchins, J. A. Covington, and D. R. Billson, Sens. Actuators A **168**, 66 (2000).
[14] M. L. Griffith and J. W. Halloran, J. Am. Ceram. Soc. **79**, 2601 (1996).
[15] F. Doreau, C. Chaput, and T. Chartier, Adv. Eng. Mater. **2**, 493 (2000).
[16] P. Singh, L. S. Smith, M. Bezdecny, M. Cheverton, J. A. Brewer, and V. Venkataramani, Proc. IEEE Int. Ultrason. Symp., p. 1111 (2011).
[17] C.-J. Bae and J. W. Halloran, Int. J. Appl. Ceram. Technol. **8**, 1289 (2011).
[18] X. N. Jiang, C. Sun, X. Zhang, B. Xu, and Y. H. Ye, Sens. Actuators A **87**, 72 (2000).
[19] J. H. Jang, S. Wang, S. M. Pilgrim, and W. A. Schulze, J. Am. Ceram. Soc. **83**, 1804 (2000).
[20] O. Dufaud and S. Corbel, Rapid Prototyping J. **8**, 83 (2002).
[21] J. Kelly, M. Leonard, C. Tantigate, and A. Safari, J. Am. Ceram. Soc. **80**, 957 (1997).
[22] E. B. Araújo, R. N. Reis, C. A. Guarany, C. T. Meneses, J. M. Sasaki, A. G. Souza Filho, and J. Mendes Filho, Mater. Chem. Phys. **104**, 40 (2007).
[23] Y. Zhang, I. S. Baturin, E. Aulbach, D. C. Lupascu, A. L. Kholkin, V. Ya. Shur, and J. Rödel, Appl. Phys. Lett. **86**, 012910 (2005).
[24] A. O'Brien, D. I. Woodward, K. Sardar, R. I. Walton, and P. A. Thomas, Appl. Phys. Lett. **101**, 142902 (2012).
[25] Q. C. Xu, S. Yoshikawa, J. R. Belsick, and R. E. Newnham, IEEE Trans. Ultrason. Ferroelectr. Freq. Contr. **38**, 634 (1991).
[26] S. Alkoy, R. J. Meyer Jr, W. J. Hughes, J. K. Cochran, Jr., and R. E. Newnham, Meas. Sci. Technol. **20**, 095204 (2009).
[27] S. Alkoy, A. Dogan, A.-C. Hladky, P. Langlet, J. K. Cochran, and R. E. Newnham, Proc. IEEE Int. Freq. Contr., p. 586 (1996).
[28] G. Mitteramskogler, R. Gmeiner, R. Felzmann, S. Gruber, C. Hofstetter, J. Stampfl, J. Ebert, W. Wachter, and J. Laubersheimer, Addit. Manuf. **1–4**, 110 (2014).
[29] K. D. Rolt, J. Acoust. Soc. Am. **87**, 1340 (1990).
[30] S. O. Leontsev and R. E. Eitel, Sci. Technol. Adv. Mater. **11**, 044302 (2010).

© 2015 The Authors. *Phys. Status Solidi A* published by WILEY–VCH Verlag GmbH & Co. KGaA, Weinheim